Journal of the Korean Magnetic Resonance Society **2005**, *9*, 122 - 137

Structural characterization of HBx-interacting protein using NMR spectroscopy

Young-Tae Lee[1], Byoungkook Kim[1], Key-Sun Kim[2] and Byong-Seok Choi[1*]

[1]Department of Chemistry and National Creative Research Initiative Center, Korea Advanced Institute of Science and Technology, 373-1, Guseong-dong, Yuseong-gu, Daejeon 305-701, Republic of Korea
[2]Biomedical Research Center, Korea Institute of Science and Technology, Cheongyang Box 131, Seoul 130-650, Republic of Korea
Received September 13, 2005

ABSTRACT : The hepatitis B virus X protein (HBx) is highly linked with liver diseases and the development of hepatocellular carcinoma. HBx-interacting protein (XIP) has been shown to abolish the transactivation functions of HBx. Here, we define the structural characteristics and HBx binding properties of XIP. Under physiological conditions, XIP was composed mainly of random-coils but significant helicity was induced in the hydrophobic condition. NMR spectroscopy defined the secondary structure of XIP in the presence of sodium dodecyl sulfate. Four putative helices were mapped to the amino acids 8-12, 32-38, 42-54 and 82-91. Any deletion of defined putative helices in XIP led to loss of binding to HBx, and truncated mutant lacking last putative helix decreased helicity more than that it could. Our results suggest that XIP requires its entire sequence for HBx binding and it may be under drastic conformational change when binds to HBx.
Key words: HBx, XIP, NMR, natively unfolded protein

INTRODUCTION

An estimated 350 million hepatitis B virus (HBV) carriers worldwide are at increased risk for the development of chronic active hepatitis (CAH), cirrhosis and hepatocellular carcinoma (HCC) [1]. HBV contains a highly conserved small open reading frame (ORF) that encodes that HBV x protein (HBx). HBx is a multifaceted protein that interacts with a wide

* To whom correspondence should be addressed. E-mail : byongseok.choi@kaist.ac.kr

variety of cellular proteins [2]. It is responsible for the pathogenesis of chronic infection and development of HCC. HBx is capable of activating many different viral and cellular promoters [3]. In addition, HBx is pleiotropic in that it serves both as a cytoplasmic activator of cell signaling cascades involving mitogen-activated protein kinase (MAPK) [4] and Janus family tyrosine kinases (JAK)/signal transducer and activators of transcription (STAT) [5] pathways and as a nuclear activator by interacting with general transcription factors such as TATA-binding protein (TBP) [6], RPB5 [7] and TFIIB [8]. HBx also binds to and inactivates negative growth-regulatory molecules, such as the tumor suppressor p53 [9, 10]. Furthermore, HBx compromises DNA repair [11, 12] and affect the normal turnover of growth-regulatory molecules in the proteasome [13]. However, the exact role of HBx is not yet clearly defined and its contribution to HCC is controversial.

Recently, an HBx-interacting protein (XIP) was identified in a hepatocellular carcinoma cell line using the yeast two-hybrid system [14]. This 9.6-kDa protein binds to HBx, abolishes the transcriptional activation properties of HBx in hepatocellular carcinoma cells, and reduces wild-type HBV replication to levels observed following transfection of HCC cell lines with an HBx-minus version of HBV. It has been proposed that in mammalian cells XIP alters the replication life cycle of HBV by binding to and inhibiting HBx. The normal physiological functions of XIP are unknown. The structural properties of XIP would not only provide insights into the HBx-XIP interaction and the physiological function of XIP, but also aid in the design of HBx-targeted drugs. In our initial step, here we report structural characterization of XIP.

MATERIALS AND METHODS

Protein expression and purification

The plasmid pGEX-4T-1-XIP, which encodes a glutathione S-transferase (GST)-XIP fusion protein, was obtained from Jongkyeong Chung (Department of Biological Sciences, Korea Advanced Institute of Science and Technology). A plasmid that encodes COOH-terminal histidine tag (His-tag) fused to XIP was constructed by inserting polymerase chain reaction (PCR)-amplified XIP DNA fragments from pGEX - 4T – 1-XIP into the NdeI-XhoI

site of the pET-21a(+) vector (Novagen). To produce a ^{15}N-labeled or $^{15}N/^{13}C$ double-labeled His-tagged XIP recombinant protein in *Escherichia coli*, the bacteria were grown in minimal media containing 6 g/L Na_2HPO_4, 3 g/L KH_2PO_4, 0.5 g/L NaCl, 1 g/L of $^{15}NH_4Cl$ (Cambridge Isotope Laboratory), 4 g/L of D-glucose (U-$^{13}C_6$ glucose for double labeling), 0.5 g/L sodium citrate, 1 g/L $MgSO_4$, 1 mL/L trace element solution and 0.65 mL/L vitamin solution was used. The trace elements and the vitamin solutions were prepared as described in Jasson *et al* [15]. XIP protein was purified on Ni-NTA resin (QIAGEN). Pooled protein was dialyzed against 50 mM ammonium bicarbonate and then lyophilized and stored –20 °C until further study.

CD spectroscopy

CD measurements were performed at room temperature with a Jasco spectropolarimetor, model J-720, using a quartz cell with the path length of 1 mm. Far-UV wavelength scans were recorded from 260 to 190 nm, with a 0.2-nm step resolution, a 50 nm/min speed, a 2-s response time, and a 1-nm bandwidth. Spectra were collected and averaged over five scans. The buffer background was subtracted from CD spectra acquired for the protein. The protein concentration was determined using the bicinchoninic acid assay. The calculation of secondary structure contents was performed with the CDNN program [16].

NMR spectroscopy

NMR experiments were carried out at 30 °C either on a Bruker DMX600 or a Varian INOVA UnityPlus 600-MHz spectrometer equipped with 5-mm inverse triple-resonance probes with z gradient coils. d_{25}-SDS (37.6 mg) was dissolved in 0.6 mL of buffer containing 50 mM sodium phosphate, pH 6.5, 3 mM DTT, 2 mM NaN_3, 0.6 mM DSS (3-(trimethylsilyl)-1-propanesulfonic acid) and 90% H_2O/10% D_2O. ^{15}N-labeled or ^{15}N, ^{13}C-double-labeled XIP (10 mg) was then dissolved in the prepared buffer. Quadrature detection was achieved with the States-TPPI method [17]. 3D CBCA(CO)NH [18] and HNCACB [19] spectra, which were used to assign backbone ^1H, ^{15}N and ^{13}C resonances, were recorded with spectral widths of 6000 Hz in F3 (^1H), 1250 Hz in F2 (^{15}N) and 8500 Hz in F1 (^{13}C). The size of the acquired matrices was (t_3, t_2, t_1) 473 (CBCA(CO)NH) and 307 (HNCACB) × 30 × 50 complex data points. The aliphatic side-chain chemical shifts of ^1H were obtained

from H(CCO)NH-TOCSY [20] and ^{15}N-NOESY HSQC. The F1 (^{1}H) spectral width of these experiments was 4500 Hz, with the size of the acquired matrices being 550 × 40 × 50 (H(CCO)NH-TOCSY) and 512 × 32 × 92 (^{15}N-NOESY HSQC), respectively. The assignment of the carbonyl carbon, CO, was carried out using HNCO [21] and HCACO [22], with carbonyl spectral widths (F1) of 2112 Hz. F2 (^{15}N, HNCO) and F2 (^{13}C, HCACO) spectral widths were set to 1250 Hz and 4524 Hz, respectively. The sizes of the acquired matrices were 512 × 28 × 56 (HNCO) and 333 × 28 × 60 (HCACO). The ^{1}H chemical shifts were given relative to DSS. The ^{15}N and ^{13}C chemical shifts were indirectly referenced from the proton dimension. The carriers were set at 4.685 ppm and 116.5 ppm for ^{1}H and ^{15}N dimension, respectively. The ^{13}C carrier was set depending on the experiment, at 46 ppm for aliphatic carbon and 174 ppm for carbonyl carbon. Data were processed on Silicon Graphics workstations using XWINNMR or NMRPipe [23]. Linear prediction was used to extend the heteronuclear dimensions to improve digital resolutions for ^{15}N-NOESY HSQC. Data analysis was performed with the Sparky program (T. D. Goddard and D. G. Kneller, Sparky, University of Californai, San Franscisco).

In vitro binding assay

[^{35}S]Methionine (Met)-labeled HBx protein was generated using the TNT quick coupled transcription/translation systems (Promega, USA). Full length of XIP and deletion mutant versions of XIP were cloned into the pGEX-4T-1 vector and expressed as GST fusion proteins, which were then purified on glutathione-Sepharose 4B resin. The [^{35}S]Met-labeled HBx protein was incubated either with XIP or the XIP deletion mutants in 200 μL of binding buffer (20 mM Tris-HCl pH 7.5, 1 mM EDTA, 110 mM NaCl, 0.1% Nonidet P-40, 0.7 μg/mL BSA, and 0.2 mM PMSF) at 4 °C for 2 h with gentle mixing. Glutathione-Sepharose 4B beads (20 μL) were added to the protein mixture, and the mixture was incubated at 4 °C for two more hours with gentle mixing. The beads were washed extensively with the binding buffer. SDS-polyacrylamide gel (PAGE) sample buffer (2X, 10 μL) was added to the beads, and boiled at 100 °C. The samples were subjected to microcentrifugation, and the supernatants were electrophoresed through a 16% SDS-PAGE. HBx binding was detected by autoradiography.

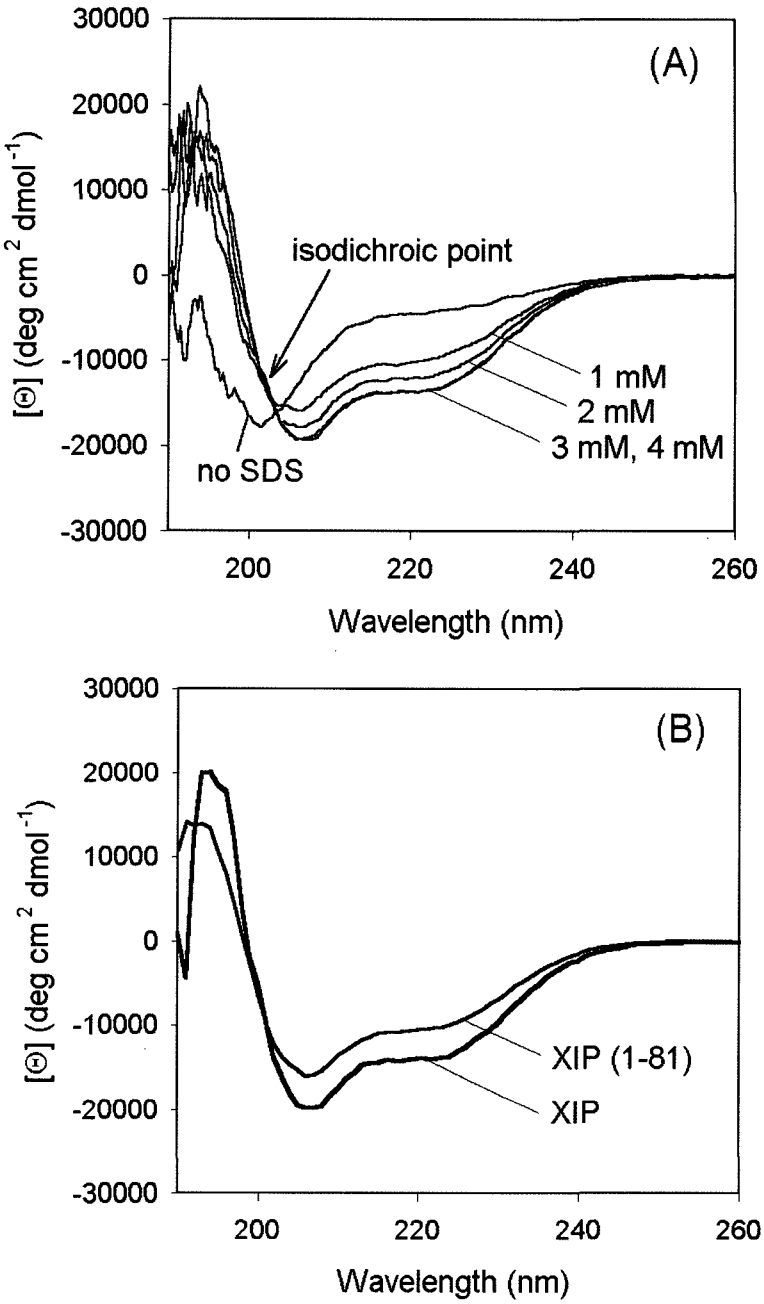

Fig. 1. CD spectra of XIP in varying concentration of SDS at pH 6.5 (A) and XIP (1-80) in 5 mM SDS (B). The concentration of XIP was 18.7 μM. The SDS concentrations on the spectrum from top to bottom are 0 mM, 1 mM, 3 mM and 4 mM. At 202 nm, an isodichroic point is observed.

RESULTS AND DISCUSSION

Under physiological conditions, CD spectra showed that XIP is composed mainly of random coils (Fig. 1A). The minimum was observed at 200 nm, and the CD decreased drastically from 210 nm, which is typically indicative of a random coil [24]. Variation of the pH from 3.5 to 8.0 did not alter the CD spectra (data not shown). This suggests that XIP is innately unfolded protein. Some proteins are unstructured in physiological condition, but fold upon forming specific complexes [25]. We were curious to see if XIP has such characteristic. However, we were not successful to produce HBx protein as others reported [26-28]. The structures of complex in synergistic folding usually involve hydrophobic interactions that stabilize complex structure [29]. Since HBx was not available, we decided to use the buffer conditions that mimic hydrophobic environment.

When trifluoroethanol (TFE), which has been used widely for stabilization of proteins [30], was added to the protein mixture, XIP started to aggregate. Detergents have both hydrophilic head group and hydrophobic alipathic group, and thus are easily solubilized in aqueous solution but make the solution hydrophobic. Addition of SDS to the protein mixture induced a structural change in XIP from random coils to an α-helical conformation (Fig. 1A) without any aggregation. As the concentration of SDS was increased, the helicity was also amplified. Maximum helicity was reached at 3 mM SDS at the given concentration of 18.7 μM of XIP. It was estimated that the helical content was ~ 40 % at 3 mM SDS. In the absence of SDS, the helical content was estimated to be ~ 10 %. Thus the addition of SDS to the protein mixture caused the helical content to increase ~ 30 %. It is noted that an isodichroic point was observed at 202 nm in the presence of SDS; however, the CD spectra obtained with 0 mM SDS did not pass this point. This suggests that a prominent structural change occurred with the initial addition of low concentration of SDS and a two-phase structural transition occurred as the concentration of SDS was increased.

NMR spectroscopy also provided evidence of a structural change in XIP upon addition of SDS. As can be seen in 1D spectra (Fig. 2A), the dispersion of amide protons was increased from 0.7 ppm in the absence of SDS to 1.3 ppm in the presence of SDS. The side chain H^{ε} proton peaks of Asp and Gln were well-resolved in the ^{15}N-HSQC spectrum (Fig. 2B). The Gly amide proton peaks upfield in the ^{15}N dimension also showed good disp-

ersion. We also observed notable line broadening of amide protons (Fig. 2A). This development of line broadening suggests that SDS molecules bound to XIP, and therefore the correlation time of the XIP-SDS complex was higher than for XIP alone.

Both CD and NMR experiments clearly indicated that SDS induces helicity in XIP. However, it remains unclear as to whether XIP is bound to individual SDS molecules or sequestered in SDS-micelles. To address this question, we performed CD experiments in the presence of small unilamellar vesicle (SUV) of phosphatidyl choline and phosphadidyl coline/phosphatidyl glycerol (2:1). The experiments showed that these lipids did not alter the conformation of XIP (data not shown). Thus it is not likely that XIP interacts with SDS-micelles. The interaction between SDS and XIP appeared to be predominately hydrophobic interactions because other detergents such as dodecylphosphocholine (DPC) produced similar CD patterns (data not shown). As DPC has a zwitter-ionic head group and SDS has a negative charge in its head group, the interaction between XIP and the two detergents does not seem to be influenced by electrostatic factors. SDS also stabilizes XIP. After the NMR sample of XIP (1 mM at pH 6.5) was prepared in the absence of SDS, XIP began to aggregate slowly. In contrast, in the presence of SDS, the protein was free from aggregation even after extensive 3D NMR experiments that took several days at 30 °C.

We performed several standard triple resonance 3D NMR experiments to assign resonances for XIP with SDS. Most of the sequential assignments were obtained from the CBCA(CO)NH and HNCACB spectra. 3D H(CCO)NH-TOCSY and ^{15}N-NOESY HSQC spectra were helpful to resolve any remaining ambiguities. Out of 114 amide resonances expected in the 2D ^{15}N-HSQC spectrum, we identified 95 main-chain amide resonances, 1 H^{ε} of Arg34 and 18 side-chain amides resonances of Asp and Gln residues. Most of the carbonyl carbon resonances except for Leu5, Glu6 and Asp58 were assigned from HNCO and HCACO spectra. The obtainment of CO, H^{α}, C^{α} and C^{β} resonances enabled the prediction of secondary structures in XIP using the CSI method [31] and the TALOS program [32]. The availability of most of backbone nuclei resonances made the prediction more accurate and also allowed quantitative analysis using the TALOS program. CSI analysis using the C^{α}, C^{β}, CO and H^{α} resonances revealed that four helical segments are present in XIP (Fig. 3). Residues 42 to 54 and 82 to 91 construct rather long α-helices, and two short helices are formed with residues 8 to 12 and 32 to 38. The third and last group of helices

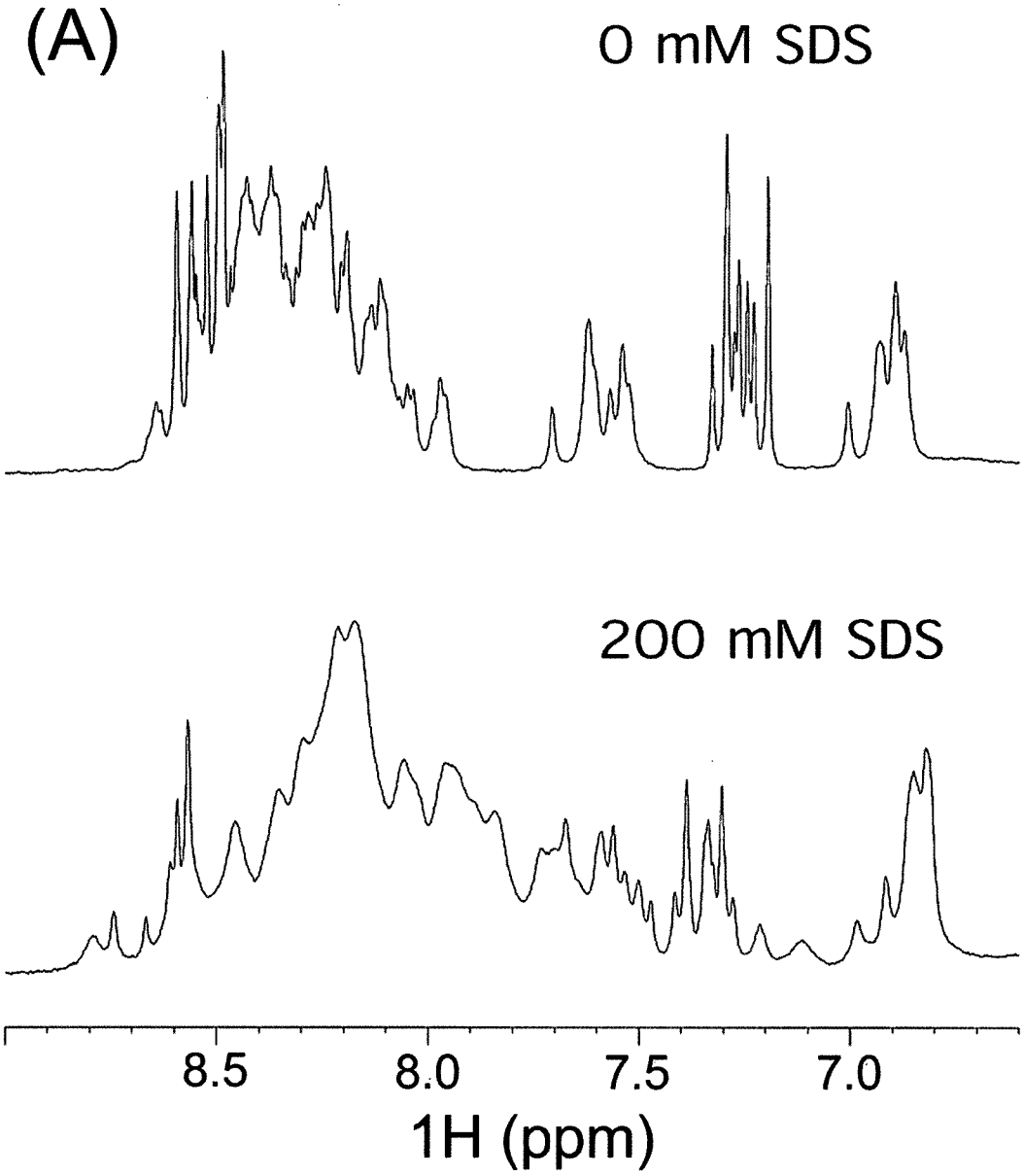

Fig. 2. ^{15}N-HSQC spectra of XIP in the absence of SDS (A) and in the presence of 200 mM SDS (B) in 50 mM sodium phosphate, pH 6.5, 3 mM DTT, 2 mM NaN_3, 0.6 mM DSS and 90 % H_2O/10 % D_2O. The cross peaks are labeled with their residue name and number. The folded in ^{15}N dimension peak from Arg34 is indicated as Arg34e. NH_2 signals from Asn and Gln side chains are connected by straight lines.

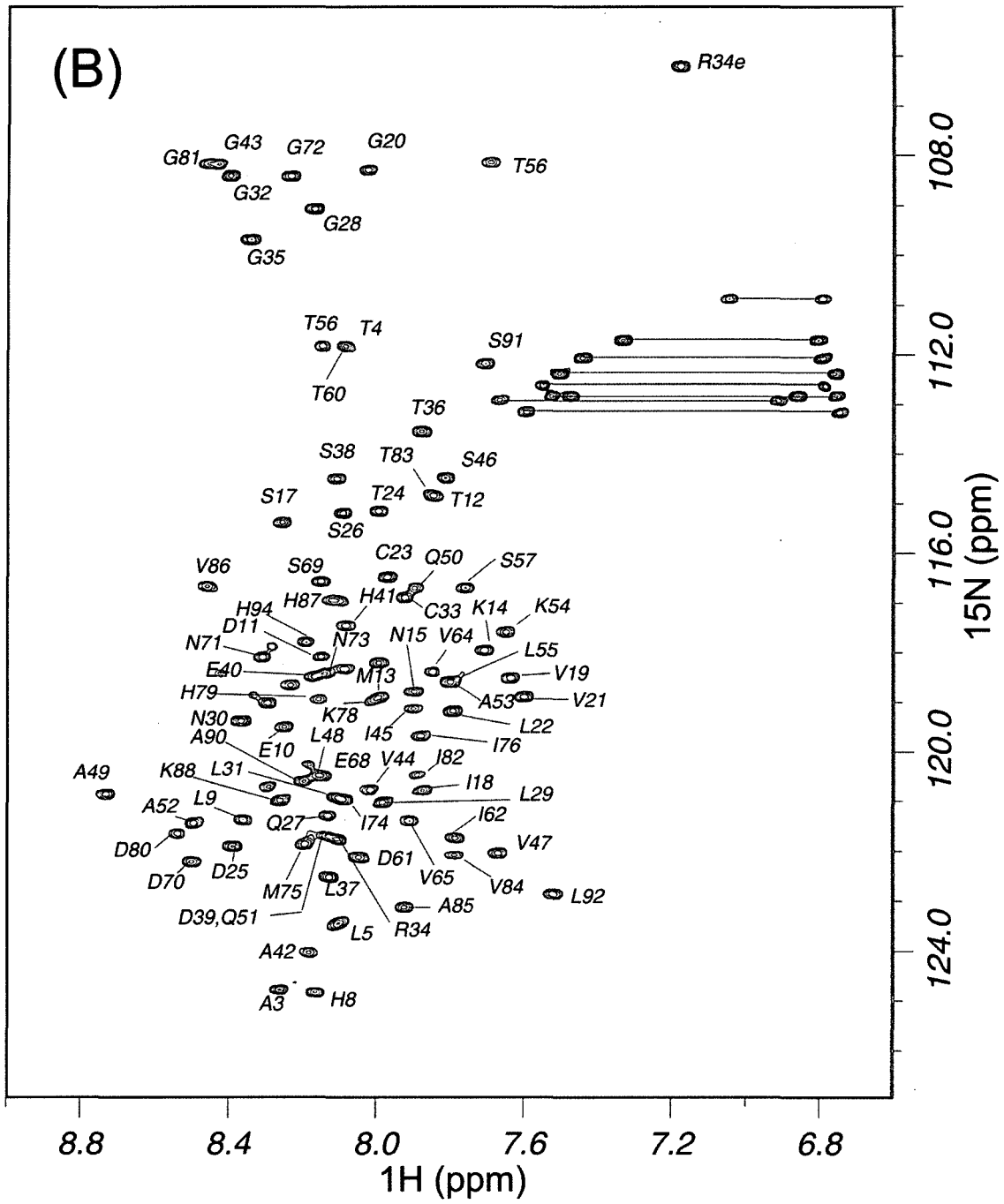

Fig. 2. continued.

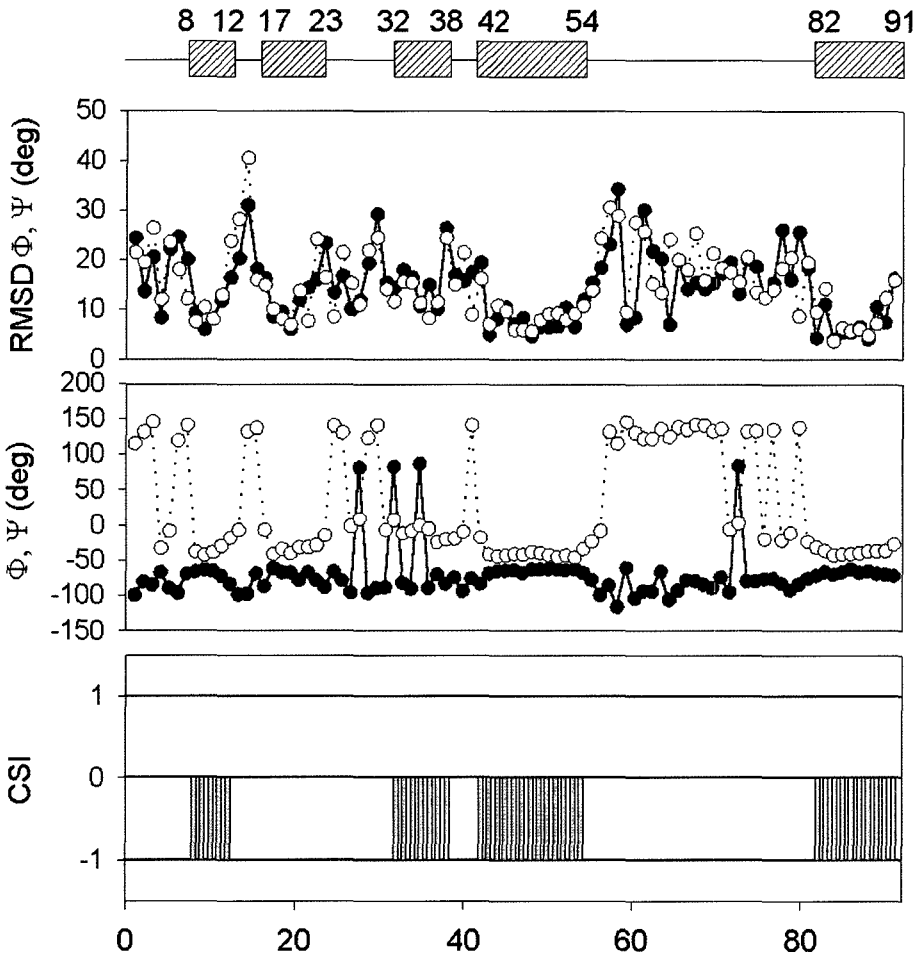

Fig. 3. Summary of structural information obtained from NMR spectroscopy. From bottom to top: consensus of CO, H^{α}, C^{α} and C^{β} CSI values; phi (filled circle) and psi (open circles) angle values predicted by the TALOS program; RMS deviation of phi (filled circles) and psi (open circles) values obtained by the TALOS program; solution secondary structure in which the α-helices are depicted by rectangles and the irregular regions by lines. The rectangle filled with coarse diagonal lines represents an α-helix predicted from the TALOS method.

predicted with the CSI method were also well defined with the TALOS approach, however, the first and second helices are somewhat poorly defined and have higher RMSDs for the Φ and ψ values. The TALOS program predicted one more helical segment between residues 17 to 23 (Fig. 3), although this helix had relatively higher RMSDs (10 to 20 deg) for the Φ and ψ values. In addition, a long β-strand in COOH-terminal half of XIP was predicted, but the RMSDs for the Φ and ψ values were much higher than the stable α-helices detected in the XIP (Fig. 3).

We asked if the whole XIP sequence is necessary or just a small region is sufficient to interact with HBx. We were especially interested in whether one of any induced helical segments is responsible for HBx binding. On the basis of the results of NMR experiments analyzed with the CSI method, several mutant versions of XIP for the *in vitro* binding assay were constructed (Fig. 4A). GST fused XIP mutants were produced in *E. coli*. Due to difficulty in the production of HBx, [^{35}S]Met-labeled HBx was produced using a coupled *in vitro* transcription-translation method. The results of the *in vitro* binding assays indicated that only intact XIP was able to interact with HBx (Fig. 4B). The interaction was abrogated by any deletion in the GST-XIP fusion protein. The HBx protein did not bind to GST alone. Taken together, these results indicated that the entire XIP amino acid sequence is required for interaction with HBx.

One of truncated XIP (1-81) mutant was expressed for the CD analysis. A helical content of 26 % was estimated for XIP (1-81) (Fig. 1B). If other helical segments were not affected by the deletion of amino acids 82 from 91, a helical content of 32 % is expected. Thus ~ 6 % of the helical content was reduced by deletion of the fourth helix. We suggest that the deletion of a helical segment might partially abrogate the tertiary folding of XIP and thus eliminate its ability to bind to HBx.

CONCLUSION

We described structural characterization of XIP in this report. XIP is unstructured in physiological condition, but folds to form four helical regions in the hydrophobic environment. Any deletion of those putative helical regions led to loss of binding to HBx,

(A)

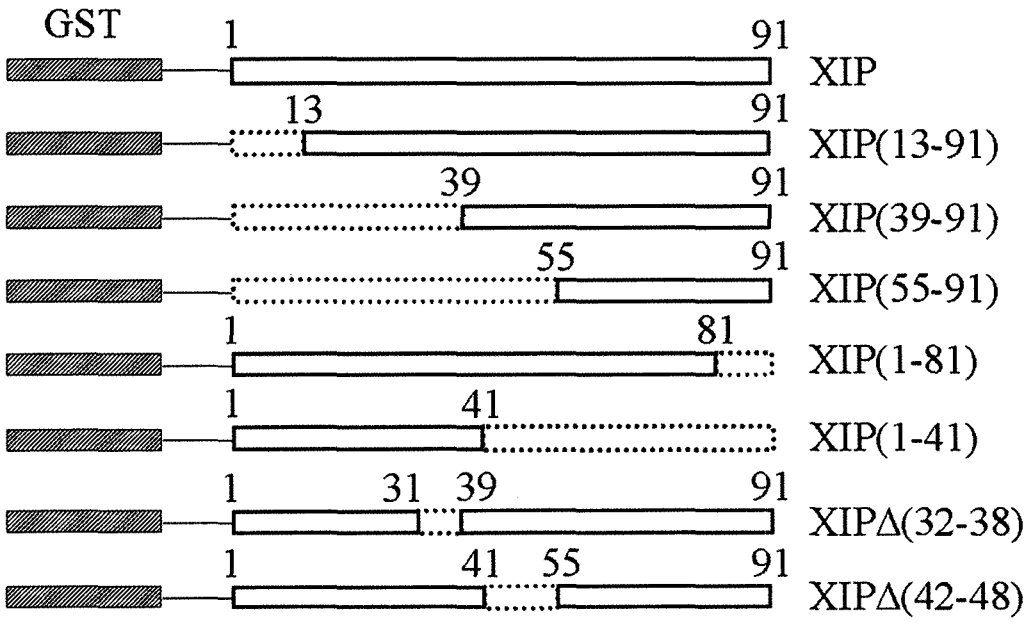

(B)

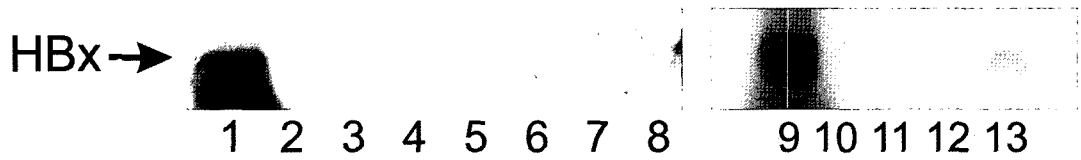

Fig. 4. Analysis of XIP binding to HBx. (A) GST-XIP fusion protein constructs. Regions 1-12, 1-38, 1-54, 82-91, 42-91, 32-38 or 42-54 of XIP were deleted. (B) Binding of [^{35}S]Met-labeled HBx to GST (lane 2 and 10), GST-XIP (13-91) (lane 3), GST-XIP (39-91) (lane 4), GST-XIP (55-91) (lane 5), GST-XIP (1-81) (lane 6), GST-XIP (1-41) (lane 7), GST-XIP (lane 8, 13), GST-XIP Δ(32-38) (lane 11), and GST-XIP Δ(42-54) (lane 12). Lanes 1 and 9 contain 20 % input of [^{35}S]Met-labeled HBx.

suggesting whole intact XIP is required for effective binding to HBx protein. Therefore we expect that conformational change would be involved in the interaction with HBx. Also HBx may go through synergistic folding with XIP. Indeed, recent structural studies on cysteine-free HBx (18-142) showed that HBx is mainly unstructured [33]. This version of HBx has been shown to retain its functional activity [34]. This structural characteristic of HBx may play a key role to interact with enormous number of cellular proteins. Further structural and interacting details of HBx and XIP should give insight into understanding the enigmatic HBx. It should be worth utilizing cystein-free HBx (18-142) for further studies, since repeated trials to produce intact HBx have been unsuccessful so far.

Acknowledgements

We thank Hana Kim for her discussions on protein-protein interactions. This work was supported by the National Creative Research Initiative Center for Repair System of Damaged DNA from the Ministry of Science and Technology, the Republic of Korea. Also, B.-K. Kim was supported partially by the BK21 project.

REFERENCES

1. P. Tiollais, C. Pourcel, and A. Dejean, "The hepatitis B virus", *Nature, 317*, 489 (1985).
2. M. J. Bouchard, and R. J. Schneider, "The enigmatic X gene of hepatitis B virus", *J Virol, 78*, 12725 (2004).
3. M. T. Rossner, "Review: hepatitis B virus X-gene product: a promiscuous transcriptional activator", *J Med Virol, 36*, 101 (1992).
4. J. Benn, F. Su, M. Doria, and R. J. Schneider, "Hepatitis B virus HBx protein induces transcription factor AP-1 by activation of extracellular signal-regulated and c-Jun N-terminal mitogen-activated protein kinases", *J Virol, 70*, 4978 (1996).
5. Y. H. Lee, and Y. Yun, "HBx protein of hepatitis B virus activates Jak1-STAT signaling", *J Biol Chem, 273*, 25510 (1998).
6. I. Qadri, H. F. Maguire, and A. Siddiqui, "Hepatitis B virus transactivator protein X interacts with the TATA-binding protein", *Proc Natl Acad Sci U S A, 92*, 1003 (1995).

7. J. H. Cheong, M. Yi, Y. Lin, and S. Murakami, "Human RPB5, a subunit shared by eukaryotic nuclear RNA polymerases, binds human hepatitis B virus X protein and may play a role in X transactivation", *Embo J, 14*, 143 (1995).
8. I. Haviv, M. Shamay, G. Doitsh, and Y. Shaul, "Hepatitis B virus pX targets TFIIB in transcription coactivation", *Mol Cell Biol, 18*, 1562 (1998).
9. R. Truant, J. Antunovic, J. Greenblatt, C. Prives, and J. A. Cromlish, "Direct interaction of the hepatitis B virus HBx protein with p53 leads to inhibition by HBx of p53 response element-directed transactivation", *J Virol, 69*, 1851 (1995).
10. L. W. Elmore, A. R. Hancock, S. F. Chang, X. W. Wang, S. Chang, C. P. Callahan, D. A. Geller, H. Will, and C. C. Harris, "Hepatitis B virus X protein and p53 tumor suppressor interactions in the modulation of apoptosis", *Proc Natl Acad Sci U S A, 94*, 14707 (1997).
11. T. H. Lee, S. J. Elledge, and J. S. Butel, "Hepatitis B virus X protein interacts with a probable cellular DNA repair protein", *J Virol, 69*, 1107 (1995).
12. S. A. Becker, T. H. Lee, J. S. Butel, and B. L. Slagle, "Hepatitis B virus X protein interferes with cellular DNA repair", *J Virol, 72*, 266 (1998).
13. J. Huang, J. Kwong, E. C. Sun, and T. J. Liang, "Proteasome complex as a potential cellular target of hepatitis B virus X protein", *J Virol, 70*, 5582 (1996).
14. M. Melegari, P. P. Scaglioni, and J. R. Wands, "Cloning and characterization of a novel hepatitis B virus x binding protein that inhibits viral replication", *J Virol, 72*, 1737 (1998).
15. M. Jansson, Y. C. Li, L. Jendeberg, S. Anderson, B. T. Montelione, and B. Nilsson, "High-level production of uniformly 15N- and 13C-enriched fusion proteins in Escherichia coli", *J Biomol NMR, 7*, 131 (1996).
16. G. Bohm, R. Muhr, and R. Jaenicke, "Quantitative analysis of protein far UV circular dichroism spectra by neural networks", *Protein Eng, 5*, 191 (1992).
17. D. Marion, M. Ikura, R. Tschudin, and A. Bax, "Rapid Recording of 2d Nmr-Spectra without Phase Cycling - Application to the Study of Hydrogen-Exchange in Proteins", *Journal of Magnetic Resonance, 85*, 393 (1989).
18. S. Grzesiek, and A. Bax, "Correlating Backbone Amide and Side-Chain Resonances in Larger Proteins by Multiple Relayed Triple Resonance Nmr", *Journal of the American*

Chemical Society, 114, 6291 (1992).

19. M. Wittekind, and L. Mueller, "Hncacb, a High-Sensitivity 3d Nmr Experiment to Correlate Amide-Proton and Nitrogen Resonances with the Alpha-Carbon and Beta-Carbon Resonances in Proteins", *Journal of Magnetic Resonance Series B, 101*, 201 (1993).
20. S. Grzesiek, J. Anglister, and A. Bax, "Correlation of Backbone Amide and Aliphatic Side-Chain Resonances in C-13/N-15-Enriched Proteins by Isotropic Mixing of C-13 Magnetization", *Journal of Magnetic Resonance Series B, 101*, 114 (1993).
21. S. Grzesiek, and A. Bax, "Improved 3d Triple-Resonance Nmr Techniques Applied to a 31-Kda Protein", *Journal of Magnetic Resonance, 96*, 432 (1992).
22. S. Grzesiek, and A. Bax, "The Origin and Removal of Artifacts in 3d Hcaco Spectra of Proteins Uniformly Enriched with C-13", *Journal of Magnetic Resonance Series B, 102*, 103 (1993).
23. F. Delaglio, S. Grzesiek, G. W. Vuister, G. Zhu, J. Pfeifer, and A. Bax, "Nmrpipe - a Multidimensional Spectral Processing System Based on Unix Pipes", *Journal of Biomolecular Nmr, 6*, 277 (1995).
24. J. T. Yang, C. S. C. Wu, and H. M. Martinez, "Calculation of Protein Conformation from Circular-Dichroism", *Methods in Enzymology, 130*, 208 (1986).
25. H. J. Dyson, and P. E. Wright, "Intrinsically unstructured proteins and their functions", *Nature Reviews Molecular Cell Biology, 6*, 197 (2005).
26. R. Truant, J. Antunovic, J. Greenblatt, C. Prives, and J. A. Cromlish, "Direct Interaction of the Hepatitis-B Virus Hbx Protein with P53 Leads to Inhibition by Hbx of P53 Response Element-Directed Transactivation", *Journal of Virology, 69*, 1851 (1995).
27. E. Hildt, P. H. Hofschneider, and S. Urban, "The role of hepatitis B virus (HBV) in the development of hepatocellular carcinoma", *Seminars in Virology, 7*, 333 (1996).
28. E. Rui, P. R. de Moura, and J. Kobarg, "Expression of deletion mutants of the hepatitis B virus protein HBx in E-coli and characterization of their RNA binding activities", *Virus Research, 74*, 59 (2001).
29. S. J. Demarest, M. Martinez-Yamout, J. Chung, H. W. Chen, W. Xu, H. J. Dyson, R. M. Evans, and P. E. Wright, "Mutual synergistic folding in recruitment of CBP/p300 by p160 nuclear receptor coactivators", *Nature, 415*, 549 (2002).

30. M. Buck, "Trifluoroethanol and colleagues: cosolvents come of age. Recent studies with peptides and proteins", *Quarterly Reviews of Biophysics, 31*, 297 (1998).
31. D. S. Wishart, and B. D. Sykes, "Chemical-Shifts as a Tool for Structure Determination", *Nuclear Magnetic Resonance, Pt C, 239*, 363 (1994).
32. G. Cornilescu, F. Delaglio, and A. Bax, "Protein backbone angle restraints from searching a database for chemical shift and sequence homology", *Journal of Biomolecular Nmr, 13*, 289 (1999).
33. E. Rui, P. R. de Moura, K. D. Goncalves, and J. Kobarg, "Expression and spectroscopic analysis of a mutant hepatitis B virus onco-protein HBx without cysteine residues", *Journal of Virological Methods, 126*, 65 (2005).
34. P. R. de Moura, E. Rui, K. D. Goncalves, and J. Kobarg, "The cysteine residues of the hepatitis B virus onco-protein HBx are not required for its interaction with RNA or with human p53", *Virus Research, 108*, 121 (2005).